PARAMETERS OF LIQUID COOLING THERMAL MANAGEMENT SYSTEM EFFECT ON THE Li-ION BATTERY TEMPERATURE DISTRIBUTION

by

Yuzhang DING[a], Minxiang WEI[a*], and Rui LIU[b]

[a] College of Energy and Power Engineering,
Nanjing University of Aeronautics and Astronautics, Nanjing, China
[b] School of Mechanical and Power Engineering, Nanjing Tech University, Nanjing, China

Original scientific paper
https://doi.org/10.2298/TSCI201019223D

In order to investigated the influence on the liquid cooling system cooling effect by changing the structural parameters, single Li-ion battery heat generation model is conducted, and used in following simulation. Subsequently, sixteen models are designed by orthogonal array, and the results are obtained by extremum difference analysis, which can quantify the influence degree, identify major and minor factors, and find the relatively optimum combination. Finally, different channel entrance lay-out is adopted to investigated. With a series of work, the effective of single battery heat generation model is proved by the discharge experiment. The coolant velocity has most evident influence on the Li-ion battery temperature rise, rectangular channel aspect ratio is second one, and the heat conducting plate thickness has the smallest influence. Similarly, for Li-ion battery temperature difference, the effect of heat conducting plate thickness and rectangular channel aspect ratio as the same, both are secondary factor, and coolant velocity is main factor. With different channel entrance lay-out, both the maximum temperatures denote a same upward trend, and better balance temperature distribution is obtained by adopt Case C system which with alternating arrange channel entrance lay-out.

Key words: liquid cooling system, orthogonal experimental, experimental, structure optimization, numerical investigation

Introduction

Nowadays, since the serious energy and environmental issues, the application of neat energy, such as electricity, is becoming the mainstream in various industry [1]. Simultaneously, for the aforementioned reasons, vehicles with traditional internal combustion engine are being replaced by the vehicles with electricity [2]. However, the energy storage with high efficiency, such as the fuel cell, supercapacitor and battery, is needed for the electrical vehicles [3]. In previous energy storages, as the energy source of the vehicles, the Li-ion battery have been paid attention by its advantages, such as high power, widely working range [4]. Whereas, according the theory of Arrhenius, the performance of Li-ion battery is easily influenced by the working conditions, for instance, the working temperature and working current. Simultaneously, in these influence factors, the working temperature is the most important factor [5]. Such as, the electrochemical reaction rate of Li-ion battery rises rapidly with the rises of working temperature, but it will cause the heat accumulation. Meantime, the capacity and maximum current

* Corresponding author, e-mail: zgwmxnuaa@126.com, weimx@nuaa.edu.cn

will be greatly reduced when Li-ion battery working at low temperature condition [6]. So the performance and security of the Li-ion battery in extreme conditions will be decreased, and the thermal behavior must be studied [7].

Due to the previous reasons, scholars carried out numerous of researches in the thermal behavior domain of Li-ion battery. With the studies, scholars found out that it is important to comprehend the principle of heat generation and exchange for thermal management system studying. As a pioneer, series of thermal modelling methods were used to predict thermal behavior by Pesaran *et al.* [8], by studying the thermodynamic behavior and the temperature nephogram, the relevance between the temperature distribution and the performance of the heat generation was obtained. Subsequently, the factors which would cause the capacity change was investigated, and a series of conclusions were obtained by Bandhauer *et al.* [9]. Through a lot of researches, they denoted that the capacity shows an extremely decreased trend when the value of the working temperature exceeded 370 K. With these continuous deepening of understanding, more researches have been proposed by scholars [10, 11], and a series of results have been obtained, all the researches are point out that a reasonable battery thermal management system is urgently needed to control battery thermal behavior.

According to the further research by the scholars, numerous battery thermal management methods have been proposed to avoid the unsafe issues of the battery. For example, use different coolant materials, such as air, water, phase change material. For air cooling, usually, scholars consider air velocity and compactness of the air-duct as the influencing factors on the thermal behavior of battery. Considering these factors, air cooling method is studied by Xun *et al*. [12], during the research, many cooling systems were adopted, the results shown that for same type of channel, enlarging the channel dimension could enhances the cooling ability but it would cause more unbalanced, and *vice versa*. Subsequently, air intake velocity, fin count, and the thickness of the fin are utilized as research factors to investigate the heat transfer ability, the optimal combination of the cooling structure for Li-ion batteries is obtained by Feng *et al.* [13], the research results show that the heat dissipation ability could improve by adopted the optimal combination. Similarly, for phase change material, its special physical properties have attracted many scholars, which can absorb or release heat during phase transition. Whereas it is unstable under a long term working due to its disadvantage of the solid state, for example low heat transfer efficiency [14, 15].

According to aforementioned paragraph, it shows that adopted air or phase change material to cooling Li-ion battery can obtain outstanding performance. However, scholars considered that compared those cooling methods, the liquid cooling could provide a stronger thermal exchange ability, and this conclusion has been verified by a series of papers [16-18]. According to the researches of the scholars which mentioned previously, it denotes that by changing the parameters of the cooling system, such as the channel type and coolant parameter, different cooling effect can be obtained. In these studies, the coolant velocity always be treated as a commonly research factor. During the study, a cooling system was investigated by Nieto *et al.* [19], simultaneously, the fitted UDF function be adopted to define the heat generation. Through a series of analyses, the results show that the maximum temperature was lower than 308.15 K when the value of the coolant rate at 2.3 Lpm. Similarly, the cooling plate thickness also be considered as a research factor, and high coolant flow rate and large cooling plate thickness could provide more powerful and balance cooling ability and keep the temperature in a low and uniform range, which was found by Tong *et al.* [20]. Simultaneously, a novel structure of the cooling plate with fin was adopted, through the research, the law between fin compactness and thermal exchange ability was obtained by the scholars [21], it shown that the interval of the

fin more tight, the ability to drop the heat source temperature more strong. Similarly, the type of cooling channel is also used as a research factor, for example the number of channel and the structure of the channel. Considering the number of the channel, a thermal behavior of the battery was obtained by Huo *et al.* [22], the results shown that increase the numbers of channel, it is equivalent to increasing the contact area between the coolant and the cooling system, which make thermal exchange ability more powerful. Furthermore, the section shape of the cooling channel is also used to study, different section shape of circular channel was investigated by Zhao *et al.* [23], with the appropriate circular channel section dimension, the cooling ability of the cooling system could stay at a powerful and efficient state. Subsequently, the irregular channel type also be considered as a research factor, such as serpentine channel. Ibrahim *et al.* [24] proposed a serpentine channel with a count of six mini-channels, and take the temperature, temperature difference, and the heat accumulation fraction as evaluation indicators. It has shown that the cooling ability is able to keep the battery pack within an appropriate temperature range for most cycling tests. Similarly, Zhang *et al.* [25] proposed a snake-type channel with a guide plate, and the results show that this snake-type channel with a guide plate possessed better thermal exchange efficiency than an ordinary snake-type channel, thus could avoiding the heat accumulation.

Through the previous description of the researches of scholars, many scholars studied the liquid cooing system with different factors, such as coolant parameters and the structure type of channel. Whereas, few scholars optimize a specific cooling system, and obtained relative optimum combination of the influencing factors. In this paper, first, it studied and fitted the heat generation curve of Li-ion battery, and then use a discharge experiment to verify it. After those researches, the orthogonal experimental is adopted, and the heat conducting plate thickness, rectangular channel aspect ratio and coolant velocity are chosen as the factors of the orthogonal design. Simultaneously, the temperature rise and the temperature difference are chosen as the indicators to analysis the influence degree and find the relatively optimum combination. After those series of work, based on the relatively optimum combination model, different channel entrance lay-out types are proposed to obtain a better cooling efficiency.

Method

Numerical models

In the studies of this paper, a series of cooling system are established, which contains many simplified components, such as, the battery module, the heat conducting plate, the cooling plate and the rectangular cooling channel, all the conformations as shown in the fig. 1. The simplified single battery model with electrodes is established by the geometric parameters of actual soft pack Li-ion battery. Also, the simplified battery module is established, which contains four pieces of single battery models, and the positive and negative electrode columns of the single battery are ignored, and the dimensions of the battery module are 200 × 133 × 36 mm.

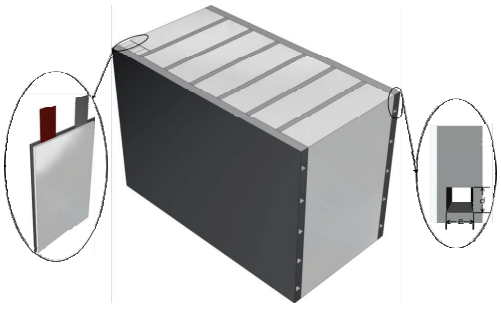

Figure 1. Liquid cooling system model

As shown in the cooling system model, it contains seven blocks of battery modules, six pieces of heat conducting plates and two pieces of cooling plates. Heat conducting plate is sandwiched between two blocks of battery modules, and a cooling plate with parallel cooling channel is vertically connected with the heat conducting plates. As shown in the figure, the

thickness of cooling plate is 10 mm, and thickness of heat conducting plate set as a variable value, L. Simultaneously, five parallel channels are located in the cooling plate, and the distribution is shown in the figure, the side length is d and e, respectively, define the channel aspect ratio as d/e.

In this article, heat conducting plate and cooling plate are assumed to be homogenous and isotropic for numerical simplicity, and aluminum is adopted for these parts. With the description of the cooling system model in previous, determine the heat conducting plate thickness, L, the rectangular channel aspect ratio, R, the coolant velocity, V, and the channel entrance lay-out are four factors effect on temperature distribution.

Equations

In this paper, the thermal models of the cooling system include three parts. First of all, a heat generation model needed; secondly, the heat conduction among the battery module, heat conducting plate and the cooling plate need to be considered; at last, the heat convection between the cooling channel surface and coolant also need to be studied.

Thermogenesis analysis

It is known from basic theory of electrochemistry, the heat generation of the Li-ion battery can be divided into four parts. First part is the chemical reaction heat, which is generated by the action that the lithium ion transferred among the positive and negative electrodes, Q_r. The second part is Joule heat, which generated due to the internal resistance of the battery, Q_J. During the process of the electrode polarization, it will produce the heat which is third part, named polarization heat, Q_p. The last part is side reaction heat Q_s, it means the electrochemical reaction heat generation, which can be neglected during calculation. Finally, after analysis, the equation of the heat generation is:

$$Q_t = Q_r + Q_J + Q_s + Q_p \tag{1}$$

Generally, the accurate heat generation rate is difficult to obtained through experiment data. So, in this article, the formula which obtained by empiric is adopted to estimate the heat generation rate during discharge, which can be expressed [26]:

$$q = \frac{1}{V_{\text{total}}}\left[I\left(E_{oc} - E\right) - IT\left(\frac{\partial E_{oc}}{\partial T}\right)\right] \tag{2}$$

where $IT(\partial E_{oc}/\partial T)$ is the equivalent to the Q_s, which can be ignored in the formula. Simultaneously, q is the heat generation rate of per unit volume, V_{total} – the battery geometric volume, I, E_{oc}, E, and T are the current, the open circuit voltage, the working voltage, and the temperature of the battery, respectively. Through the previously mentioned studies, the fitted heat generation rate curves which varies with the state of charge (SOC) is obtained, and the equation of the fitted curves under 1C and 2C discharge rate are shown as follows, it is a fitting formula which related to SOC:

$$Q = 10^6 \cdot \cdot\left(0.859SOC^6 - 2.926SOC^5 + 4.08SOC^4 - 2.995SOC^3 + 1.23SOC^2 - 0.281SOC + 0.04048\right) \tag{3}$$

$$Q = 10^7 \cdot \cdot\left(0.343SOC^6 - 1.169SOC^5 + 1.63SOC^4 - 1.197SOC^3 + 0.491SOC^2 - 0.112SOC + 0.01619\right) \tag{4}$$

Thermal transfer analysis

As described in previous section, thermal transfer in this paper can be divided into two categories, one part is the thermal conduction among the solids, and the other part is the thermal convection among the solid and liquid. With the deep understanding, the steady heat conduction and the heat convection equations are shown:

$$Q = \frac{A}{\delta}\left(T_{\mathrm{h}} - T_{\mathrm{c}}\right) \tag{5}$$

$$\phi = hA\left(T_{\mathrm{w}} - T_{\mathrm{f}}\right) \tag{6}$$

where Q and ϕ are the heat transfer between the domain, T_{h} and T_{c} – the temperature of the heat conducting plate and cooling plate, T_{w} and T_{f} – the temperature of the cooling channel surface and the coolant, respectively, A – the contact area between the domain, and h – the convective heat transfer coefficient.

Results and discussions

Single Li-ion battery temperature distribution

In this section, simplified single battery model is studied, and the model is shown in fig. 1, through experiment and simulation under 1C discharge rate, the obtained results are shown in fig. 2. Analyzing the results, it can find out that the positive electrode possesses the highest average temperature, and the value is 306.33 K. Simultaneously, the average temperature of the negative electrode reaches 304.89 K, which is lower than that of the positive electrode. The lowest average temperature located at core domain of the battery, which the value is 303.72 K, compared with the average temperature of the electrodes, it is reduced by 2.31 K, 1.14 K, respectively. It is because considerable heat will be generated by the positive electrode, and the negative electrode heat generation ability is weaker than that of the positive electrode, cause the thermal behavior appeared which described in previous section.

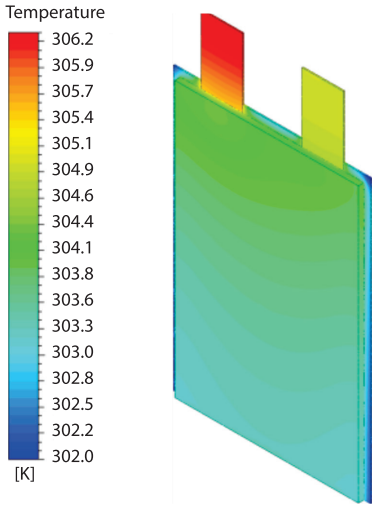

Figure 2. Single Li-ion battery temperature nephogram

To verify the accuracy of the model which studied in this paper, three points on the single battery surface are monitored to get the value of the temperature change during the experiment and simulation, named Points 1-3. Subsequently, the obtained temperature curves are shown in fig. 3.

It is shown in the figure, the temperature curves rise rapidly when the battery in the early stage of discharge. Subsequently, the change tendency of the curves is slow down during the discharge time which between 800 seconds and 3200 seconds. When the discharge is nearing the end, the value of battery SOC is nearly 0, which

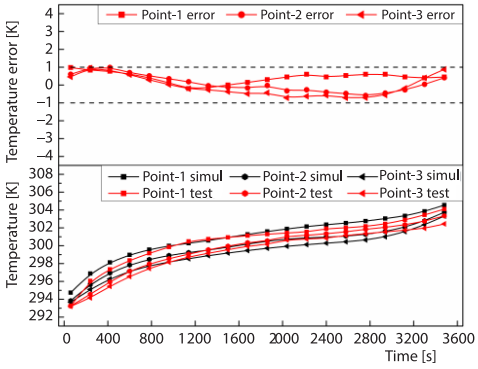

Figure 3. Simulation results and experimental results

make the Li-ion battery internal resistance increased, finally cause the temperature curves rise rapidly again. Simultaneously, as shown in the figure, the simulation results shown same trend with the experimental results, and the value of the difference of the results is less than 1 K, it considered that the model which established in previous section is precise and effective.

Orthogonal experimental scheme and analysis

This section investigated the effects of three factors: the heat conducting plate thickness, the rectangular channel aspect ratio, the coolant velocity, namely L, R, and V. In this chapter, different factor combinations are used for orthogonal experimental scheme, and the interaction between the factors need to be ignored to simplify the design of experimental. Subsequently, different levels of each factor are quantified within a reasonable rang. Considering the research content of this paper, stipulate the object of the optimization program is to lower the battery temperature and temperature difference, and the battery pack temperature rise and temperature difference are chosen as the evaluation indicators.

In this article, three factors are investigated, each factor included four levels. Different levels of the heat conducting plate thickness be selected, ranging from 4-10, respectively: 4, 6, 8, and 10. Similarly, rectangular channel aspect ratio is divided in four levels: 1, 3, 5, and 7. The levels of coolant velocity are 0.04 m/s, 0.08 m/s, 0.12 m/s, and 0.16 m/s. Factor combinations are obtained by orthogonal table to reduce the workload. As shown in tab. 1, the numbers which from 1-16 are represented the sixteen types of case, and four levels of each factor with equal frequency of occurrence.

Table 1. Orthogonal design table and evaluation indexes

Model	L [mm]	R	V [ms^{-1}]	Indicator, A [K]	Indicator, B [K]
1	4	1	0.04	10.75	6.64
2	4	3	0.16	7.58	4.83
3	4	5	0.12	6.91	5.05
4	4	7	0.08	8.49	5.5
5	6	1	0.08	8.79	5.43
6	6	3	0.04	10.54	6.54
7	6	5	0.16	6.91	4.84
8	6	7	0.12	6.54	5.08
9	8	1	0.12	8.16	5.05
10	8	3	0.08	8.59	5.49
11	8	5	0.04	9.1	6.96
12	8	7	0.16	6.22	4.82
13	10	1	0.16	7.01	4.94
14	10	3	0.12	6.94	5.14
15	10	5	0.08	7.31	5.55
16	10	7	0.04	8.81	7.02

With aforementioned work, the orthogonal table is obtained by use the theory of orthogonal design, and it is used to arrange the factors and levels of the cooling system model, which denote in tab. 1. In the table, indicator A and indicator B are the temperature rise and the temperature difference of the battery pack. With a series of work, tabs. 2 and 3 are obtained by

analysis the data in the tab. 1. As shown in the tables, the X_{ct} is the sum of the temperature rise and the Y_{dt} – the sum of the temperature difference. Similarly, S_c and S_d and are the mean square deviation of the temperature rise and temperature difference, respectively.

Table 2. Range analysis of the evaluation index *A*

Evaluation index, *A*	*L*	*R*	*V*
X_{c1} [K]	33.73	34.71	39.20
X_{c2} [K]	32.78	33.65	33.18
X_{c3} [K]	32.07	30.23	28.55
X_{c4} [K]	30.07	30.06	27.72
S_c	0.34	0.51	1.14

Table 3. Range analysis of the evaluation index *B*

Evaluation index, *B*	*L*	*R*	*V*
Y_{d1}[K]	22.02	22.06	27.16
Y_{d2} [K]	21.89	22.00	22.06
Y_{d3} [K]	22.32	22.40	20.32
Y_{d4} [K]	22.65	22.42	19.43
S_d	0.07	0.05	0.75

As shown in fig. 4(a), heat conducting plate thickness is increased from 4-10 mm, the temperature rise curve shows a steady downward trend. The value of temperature rise is decreased from 8.43 K, and the minimum value is reached 7.52 K while the thickness is 10 mm. It is because increase the heat conducting plate thickness will increase the contact area. According to the eq. (5), increase the contact area can improve the thermal transfer ability, make more heat is transferred between the plates, and decrease temperature rise.

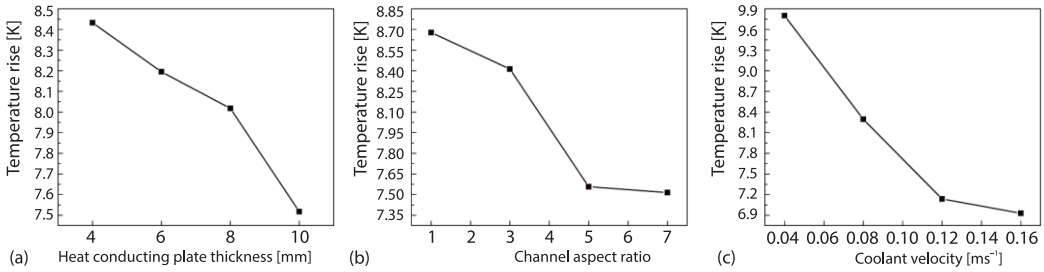

Figure 4. Effect of factors with different levels on temperature rise; (a) heat conducting plate, (b) rectangular channel aspect ratio, and (c) coolant velocity

Also, as shown in fig. 5(a), when heat conducting plate thickness is increased from 4-6 mm, the value of the temperature difference decreased from 5.51-5.47 K. In contrast, when the thickness is increased from 6-10 mm, there is an obvious increase of the temperature difference. While the value of the thickness is 10 mm, the contact area between plates is increased compared with that when the value of the thickness is 6 mm. But the heat conducting plate

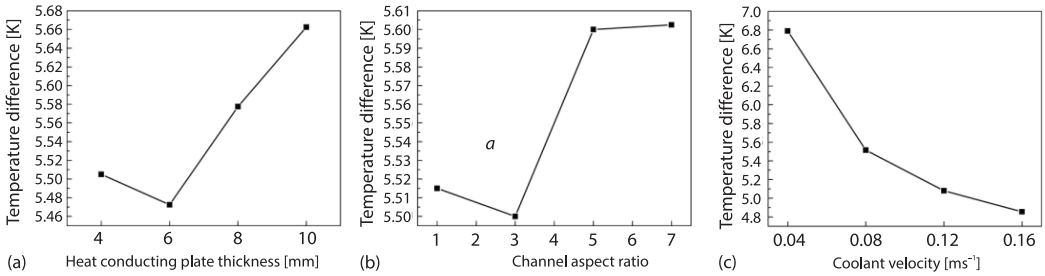

Figure 5. Effect of factors with different levels on temperature difference; (a) heat conducting plate, (b) rectangular channel aspect ratio, and (c) coolant velocity

structure and the cooling plate structure uneven matching, resulting unbalanced cooling efficiency of the cooling system, thus make the temperature distribution is inhomogeneous.

In this paper, rectangular channel aspect ratio is increased from 1-7, and the temperature rise curve is shown in fig. 4(b), it is dropped from the 8.68 K. It denotes in the figure, when rectangular channel aspect ratio is increased from 3-5, the battery temperature rise drop is most obvious. As shown in fig. 5(b), the value of temperature difference decreased from 5.52-5.5 K when the rectangular channel aspect ratio is increased from 1-3. However, when rectangular channel aspect ratio is changed from 3-5, the temperature difference increased from 5.5-5.6 K, subsequently, the temperature difference increase tendency tends to be gentle while rectangular channel aspect ratio is changed from 5-9. It is because the perimeter of the rectangular channel is increased with the aspect ratio increase under the same cross-sectional area, which make the contact area increased. It can be seen from the eq. (6), increase the contact area is beneficial to enhance the heat exchange ability between the cooling channel and coolant.

In the figs. 4(c) and 5(c), the temperature rise is decreased from 9.8-6.93 K when the coolant velocity is changed from 0.04-0.16 m/s. Similarly, the temperature difference is decreased from 6.79-4.86 K under the same work condition. Both the lowest temperature rise and the lowest temperature difference are obtained when coolant velocity set as 0.16 m/s in the simulation. This is due to the gradual increase of the coolant velocity will result gradual increase of the heat exchange ability, thereby decreased the temperature rise and temperature difference of the battery pack.

The correspondence between factors and the mean square deviation of the temperature rise and temperature difference is obtained by a series of calculations, and display in the fig. 6. In the figure, the factors, placed on the abscissa, such as *L*, *R*, and *V*. The ordinate is the value of mean square deviation of the temperature rise and temperature difference. When the value of the mean square deviation is larger, according to the theory of mathematical statistics, it means that the factor has more great effect on evaluation indicator.

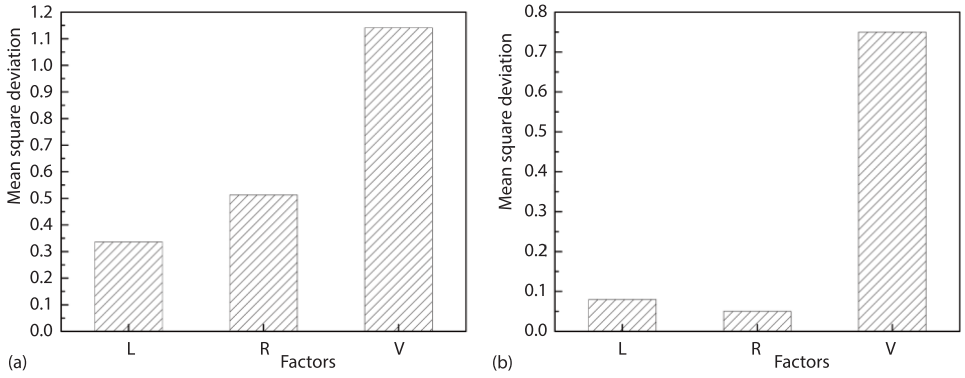

Figure 6. Mean square deviation of factors; (a) temperature rise and (b) temperature difference

Through the previous analysis, based on the data in figs. 4-6, the Model 17 is obtained, which is the relative optimum levels of each factor on cooling system, and the parameters are selected: the heat conducting plate thickness is 10 mm, the rectangular channel aspect ratio is 5, and the coolant velocity is 0.16 m/s.

Also, the temperature rises and temperature differences of the battery pack are obtained by a series of simulations, which shown in fig. 7. The figure denote that the temperature rise of the Model 17 is lower than that of all the models which in the orthogonal design table. It

also denotes that the cooling system Model 17 has evident advantage to reduce the battery pack temperature difference.

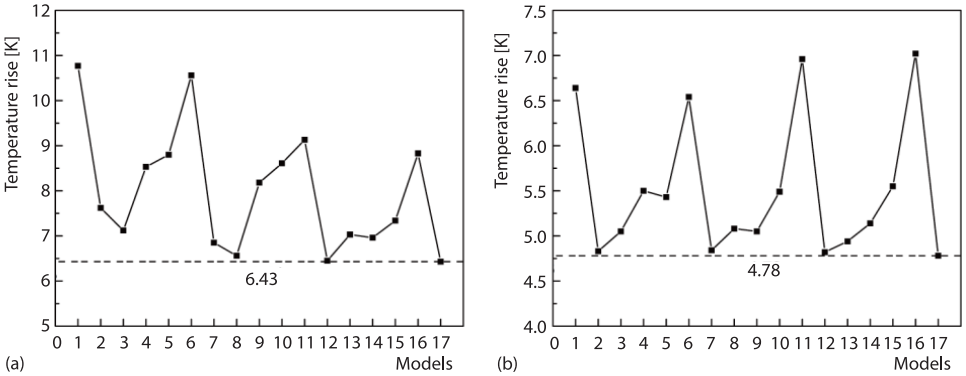

Figure 7. Comparison of different models; (a) temperature rise comparison of different models and (b) temperature difference comparison of different models

Model performance analysis with different channel entrance lay-out

In this section, to investigate the battery pack temperature phenomenon with different channel entrance lay-out, the structure of the cooling system Model 17 is used for study, subsequently, three types of entrance lay-out are proposed which is named by Case A, B, and C. In these lay-outs, the Case A system used a structure which contain a unilateral channel entrance, it means that the coolant in cooling channel flows in the same direction. In contrast, the channel entrance lay-out of the Case B cooling system possess another type, in this type of lay-out, the entrance of the three cooling channels which placed at the center part of the plate, is different from the other two cooling channel. Subsequently, a novel alternate arrange entrance lay-out is used in the Case C system, it means that the coolant possess an inverse direction which flow through in the adjacent channels.

Through simulation, temperature nephogram with different entrance lay-out as shown in fig. 8, it shows a evident temperature characteristic under 2C discharge rate. As shown in the figure, the temperature rises are basically as the same while Cases B and C systems are adopted, which the value are 6.14 K, 6.18 K, respectively. In contrast, the temperature rise is the largest one while Case A cooling system is used, and the value of the temperature rise reaching 6.46 K. Similarly, the figure denotes that the thermal behavior which use the Case A cooling system is most unbalance, and the value of the temperature difference is 4.8 K when the iteration of discharge finish. The Case B and C cooling system possess a relatively balanced heat transfer ability, when these cooling systems are used to cooling the battery pack, the values of the temperature difference are 4.4 K and 4.33 K, respectively. Compared with the temperature difference when the Case A system is used, the values of that are reduced by 0.4 K, 0.47 K, respectively. Which cause of this phenomenon is due to the different flow directions of the coolant in the cooling channel. In this section, the

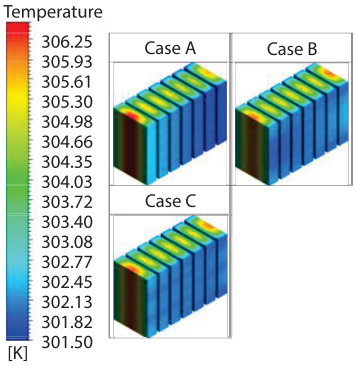

Figure 8. Temperature nephogram with different channel entrance lay-out

channel entrances of the Case A system are arranged unilateral and make the coolant in all channel flows in the same direction. Therefore, as the coolant temperature increases, heat accumulation occurred at the second half of the battery pack, make the temperature consistency worse. In contrast, the alternating arrange entrance lay-out is used in the Case C cooling system, which make the thermal exchange ability at both ends are basically equal, as a result, the temperature of the battery pack using this system is the most balanced.

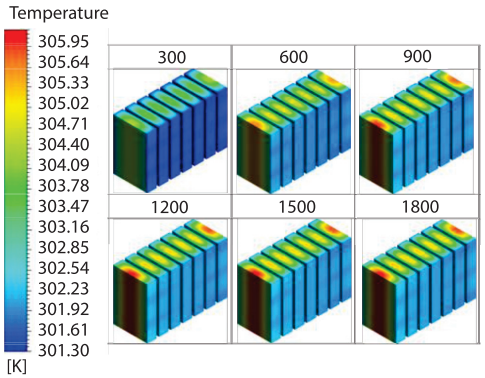

Figure 9. Temperature nephogram of Li-ion battery for Case C at different time

Also, the temperature nephogram which varying with discharge time are studied in this section, different time be selected, ranging from 300-1800 seconds, respectively: 300 second, 600 second, 900 second, 1200 second, 1500 second, and 1800 second. Assumed the battery discharged at the 2C rate, and Case C cooling system is chosen to perform thermal control, the obtained nephogram are shown in fig. 9. From the figure, as the iteration progresses, the change of the temperature nephogram becomes unobvious after 900 seconds. Simultaneously, the temperature of the battery module is gradually increased along the flow direction, and in the battery pack, series of high temperature domains are emerged due to the thermal exchange efficiency is reduced on the coolant flow direction.

Conclusion

In this study, Li-ion battery temperature shows a fast rise trend during discharge, compared to the temperature of the part which near the electrodes, the temperature is much lower in the other part of the battery. Simultaneously, in these two pieces of electrodes, the average temperature of negative electrode is lower. For Li-ion battery pack temperature rise, the effect of coolant velocity is most obvious, followed by the effect of rectangular channel aspect ratio, and the heat conducting plate thickness has minimum effect. Similarly, for the temperature difference, the effect of heat conducting plate thickness and rectangular channel aspect ratio are similar, both are the secondary influencing factor, and the coolant velocity is main factor. After analysis, a relatively optimum combination is obtained, and named Model 17, its temperature rise and temperature difference are lowest in all models. Finally, the battery pack with a series of cooling systems which have distinct entrance lay-out are studied, which show a similar change trend of the temperature change. In those studies, by adopted the Case C cooling system which with a alternating arrange entrance lay-out type, most balance temperature distribution can obtained.

Acknowledgment

This study was funded by the Jiangsu Province Key Laboratory of Aerospace Power System (Grant No. CEPE2018003), and the research project was also supported by the Introduce Talent Funding for Scientific Research at Nanjing Tech University (Grant No. 3827401744).

References

[1] Fathabadi, H., High Thermal Performance Lithium-Ion Battery Pack Including Hybrid Active-Passive Thermal Management System for Using in Hybrid/Electric Vehicles, *Energy, 70* (2014), 1, pp. 529-538

[2] Williams, B. D., *et al.*, Commercializing Light-Duty Plug-in/Plug-out Hydrogen-Fuel-Cell Vehicles: Mobile Electricity Technologies and Opportunities, *Journal of power sources, 166* (2007), 2, pp. 549-566
[3] Song, Z., *et al.*, The Battery-Supercapacitor Hybrid Energy Storage System in Electric Vehicle Applications: A Case Study, *Energy, 154* (2018), 1, pp. 433-441
[4] Yuhong, O., *et al.*, Nanoscale Interface Control for High-Performance Li-Ion Batteries, *Electronic Materials Letters, 8* (2012), 2, pp. 91-105
[5] Linda, A. W., *et al.*, Life Cycle Assessment of a Lithium-Ion Battery Vehicle Pack, *Journal of industrial ecology, 18* (2014), 1, pp. 113-124
[6] Boynuegri, A. R., et al., A New Perspective in Grid Connection of Electric Vehicles: Different Operating modes for elimination of energy quality problems, *Applied Energy*, *132* (2014), 11, pp. 435-451
[7] Al-Hallaj, S., Selman, J. R., Thermal Modelling of Secondary Lithium Batteries for Electric Vehicle/Hybrid Electric Vehicle Applications, *Journal of Power Sources*, *110* (2002), 2, pp. 341-348
[8] Pesaran, A. A., Battery Thermal Models for Hybrid Vehicle Simulations, *Journal of Power Sources*, *110* (2002), 2, pp. 377-382
[9] Bandhauer, T. M., *et al*., A Critical Review of Thermal Issues in Lithium-Ion Batteries, *Journal of the Electrochemical Society*, *158* (2011), 3, pp. 1-25
[10] Rao, Z. H., *et al.*, Thermal Management of Cylindrical Power Battery Module for Extending the Life of New Energy Electric Vehicles, *Applied Thermal Engineering*, *85* (2015), 1, pp. 33-43
[11] Rao, Z. H., *et al.*, Experimental Investigation on Thermal Management of Electric Vehicle Battery with Heat Pipe, *Energy Conversion and Management*, *65* (2013), 1, pp. 92-97
[12] Xun, J. Z., *et al.*, Numerical and Analytical Modelling of Lithium Ion Battery Thermal Behaviors with Different Cooling Designs, *Journal of Power Sources*, *233* (2013), 1, pp. 47-61
[13] Feng, X. L., *Hu, J.*, Analysis and Optimization Control of Finned Heat Dissipation Performance for Auto-Mobile Power Lithium Battery Pack, *Thermal Science*, *24* (2020), 5B, pp. 3405-3412
[14] Qu, Z. G., *et al*., Numerical Model of the Passive Thermal Management System for High-Power Lithium Ion Battery by Using Porous Metal Foam Saturated with Phase Change Material, *International Journal of Hydrogen Energy*, *39* (2014), 8, pp. 3904-3913
[15] Samimi, F., *et al*., Thermal Management Analysis of a Li-Ion Battery Cell Using Phase Change Material Loaded with Carbon Fibers, *Energy*, *96* (2016), Feb., pp. 355-371
[16] Nelson, P., *et al*., Modelling Thermal Management of Lithium-Ion PNGV Batteries, *Journal of Power Sources*, *110* (2002), 2, pp. 349-356
[17] Liu, R., *et al*., Numerical Investigation of Thermal Behaviors in Li-ion Battery Stack Discharge, *Applied Energy*, *132* (2014), 11, pp. 288-297
[18] Zhang, Y. P., *et al*., Thermal Performance Study of Integrated Cold Plate with Power Module, *Applied Thermal Engineering*, *29* (2009), 17, pp. 3568-3573
[19] Nieto, N., *et al*., Novel Thermal Management System Design Methodology for Power Lithium-Ion Battery, *Journal of Power Sources*, *272* (2014), 12, pp. 291-302
[20] Tong, W., *et al.*, Numerical Investigation of Water Cooling for a Lithium-Ion Bipolar Battery Pack, *International Journal of Thermal Sciences*, *94* (2015), 1, pp. 259-269
[21] Jin, L.W., *et al.*, Ultra-Thin Minichannel LCP for EV Battery Thermal Management, *Applied Energy*, *113* (2014), 1, pp. 1786-1794
[22] Huo, Y., *et al*., Investigation of Power Battery Thermal Management by Using Mini-Channel Cold Plate, *Energy Conversion and Management*, *89* (2015), 1, pp. 387-395
[23] Zhao, J. T., *et al*., Thermal Performance of Mini-cChannel Liquid Cooled Cylinder Based Battery Thermal Management for Cylindrical Lithium-Ion Power Battery, *Energy Conversion and Management*, *103* (2015), 10, pp. 157-165
[24] Ibrahim, A., *et al*., Performance of Serpentine Channel Based Li-on Battery Thermal Management System: An Experimental Investigation, *International Journal of Energy Research*, *44* (2020), 13, pp. 10023-10043
[25] Zhang, Y. P., *et al*., Thermal Performance Study of Integrated Cold Plate with Power Module, *Applied Thermal Engineering*, *29* (2009), 17, pp. 3568-3573
[26] Bernardi, D., *et al*., General Energy-Balance for Battery Systems, *Journal of The Electrochemical Society*, *132* (1985), 1, pp. 5-12

Paper submitted: October 19, 2020
Paper revised: June 9, 2021
Paper accepted: June 11, 2021